Image Processing and Behaviour Planning for Intelligent Vehicles

T. Bücher, C. Curio, J. Edelbrunner, C. Igel, D. Kastrup, I. Leefken, G. Lorenz, A. Steinhage, and W. von Seelen

Abstract— **Since the potential of soft-computing for driver assistance systems has been recognized, much effort has been spent in the development of appropriate techniques for robust lane detection, object classification, tracking, and representation of task relevant objects. For such systems in order to be able to perform their tasks the environment must be sensed by one or more sensors. Usually a complex processing, fusion, and interpretation of the sensor data is required and imposes a modular architecture for the overall system. In this paper, we present specific approaches considering the main components of such systems. We concentrate on image processing as the main source of relevant object information, representation and fusion of data that might arise from different sensors, and behaviour planning and generation as a basis for autonomous driving. Within our system components most paradigms of soft-computing are employed; in this article we focus on Kalman-Filtering for sensor fusion, Neural Field dynamics for behaviour generation, and Evolutionary Algorithms for optimization of parts of the system.**

Keywords— **Driver Assistance Systems, Real-time Computer Vision, Vehicle and Lane Detection, Pedestrian Recognition, Context based Object Recognition, Data Representation, Behaviour Planning and Generation, Intelligent Vehicles**

I. Introduction

Driver assistance systems aim at increasing the comfort and safety of traffic participants by sensing the environment, analysing the situation and signaling relevant information to the driver. In order to reliably accomplish this demanding task, the information of different sensors must be evaluated and fused to obtain a suitable representation of the traffic situation. The complexity of the whole data processing architecture is determined by actual task the driver assistance system is devoted to. Among others, these tasks include lane departure warning, lane keeping, collision warning or avoidance, adaptive cruise control, and low speed automation in congested traffic.

Despite their different behaviours, driver assistance systems share a common architecture as well as common specialized data processing algorithms. From an industrial point of view a modular and extensible architecture is highly appreciated, due to the simplification of the implementation of the different system tasks. In this paper, we put forward our architecture and some key components of which driver assistance systems consist. The architecture (fig. 1) is organized in four layers: a preprocessing layer, a layer consisting of domain specific processing modules, an integrating representation of the scene, and a reasoning layer working on behaviour planning or warning. In the image processing stage relevant objects are extracted from the video data stream. The geometric object informations are transformed to world coordinates and are further processed in the representation of the scene. At this stage the information about the relevant objects observed by the image processing stage can be fused with data stemming from other sensors, like RADAR or LIDAR. The representation is then accessed by the higher level modules, implementing the actual task, i.e., the demanded behaviour of the system.

The authors are with the Institut für Neuroinformatik, Ruhr-Universität Bochum, Germany. E-mail: Thomas.Buecher@neuroinformatik.ruhr-uni-bochum.de.

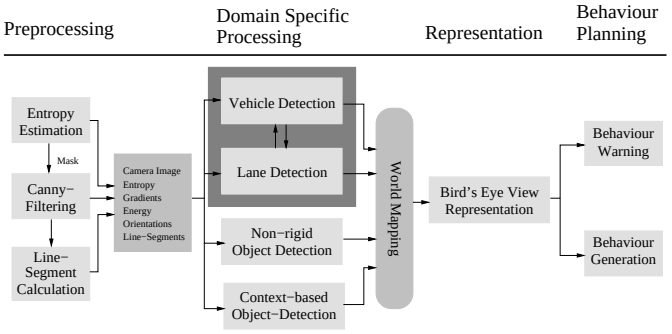

Fig. 1. Components of our driver assistance system. In the pre- and domain specific processing our image analysis components are depicted. Further sensors like RADAR and LIDAR may provide physical measurements that will be processed in these stages. The representation aims at fusing these informations with the image data based scene description.

The organisation of this paper follows figure 1. At first, image analysis including the preprocessing and domain specific processing, is presented in detail in section II. In this section, it is demonstrated how the combination of domain knowledge, imbedded by a flexible road lane estimation mechanism and the coupling with object detection modules, exploiting temporal redundancies, yield accurate descriptions of scene elements. In section II-E we focus in particular on pedestrian recognition in urban environments. In section II-F we present our work on how to incorporate domain knowledge into the interpretation process of segmentation results, here based on color features.

Working on the results of the image processing stage, in section III an approach is presented for fusing additional sensor data within an integrating array of Kalman filters.

Our work on behaviour generation, presented in section IV, is motivated by the following issues. Being able to autonomously generate a variety of basic driving behaviours, the actual driver's manoeuvre can be judged by dynamically comparing the scene as observed by the sensing sys-

tem with potential driving manoeuvres, as would be generated by the behaviour generation stage. On that basis it should be possible to calculate a risk associated with the current situation.

II. Image Processing for Driver Assistance

Research on vision-guided vehicles has become an important subject in the last decade. This is reflected by a number of government as well as industry initiated research projects and conferences. Most work has been done in the field of detection, classification and tracking of task relevant objects [1], [2], [3], [4], [5], [6], [7]. In the references [8], [9] an overview about projects demonstrating long distance autonomous driving is given.

A widely recognized approach to lane detection is presented in [10]. In this approach, a dynamical model consisting of three almost decoupled subsystems is linked to spatial motion in an extended Kalman-Filtering approach. Within the subsystems, horizontal as well as vertical road curvature and the lateral lane offset of the vehicle are recursivly estimated. The GOLD system [1] aims at autonomous driving and has been tested on some thousands of kilometers on extra-urban roads. Both lane and vehicle detection are based on inverse perspective mapping, which is performed on a special purpose hardware in real-time. In this system no temporal continuity is exploited and results of the image processing are directly used for controlling the vehicle, i.e., there is no intermediate representation of the observed scene. In a number of papers different aspects of the EMS-Vision (expectation based multifocal saccadic vision) system are described [11], [12], [13], but in contrast to our work the focus is put on software design issues. In [14] a system for real-time vehicle and lane detection is presented. Here, real-time processing is obtained by relying only on the grey-level intensity image, i.e., no image features are calculated.

In contrast to most of these approaches, our goal is to provide a complete scene representation, on the basis of which the actual task of the driver assistance system can be implemented. For this reason we calculate high level image features, by which the development of the domain specific image processing modules is significantly simplified. The presented system serves as a fundamental image processing basis for a number of 'Intelligent Vehicles' projects carried out in collaboration with industry partners. For this reason the architecture must benefit the development of different driver assistance applications by providing the task relevant information in a world-coordinate system based scene representation, which can be read out by the modules realizing the driver assistance task.

In the following, we will give an overview about the preprocessing, the higher level image processing modules, and the strategies for integrating lane and vehicle hypotheses.

A. Preprocessing

The image features calculated in the preprocessing stage should be meaningful and accurately estimated, while computation time is restricted. To meet this requirement we compute a pixel mask, to which the subsequent image processing operations will be restricted. This mask is obtained by adaptive thresholding of an estimated[1] entropy image. By applying the pixel mask we efficiently calculate local image orientations and line-segments on the basis of a Canny-Edge-Detector [15]. The line-segments are obtained by clustering pixel chains having identical orientations. Each segment is characterized by the pixel coordinates of its end-points and the mean gradient along that segment, and therefore it provides a sparse coding of the image contours.

We believe that the calculation of these high level features are beneficial for at least two important reasons: On the hand the development of the task specific modules based on these features is significantly simplified, and on the other hand they are less sensitive to varying lightning conditions and noise. Even the computation required for the whole image processing can be reduced, due to less costly processing in the higher level modules, as demonstrated further below.

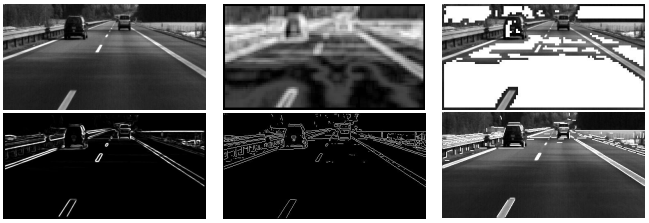

Fig. 2. Results of the preprocessing stage. Top row: camera image and entropy image, Center Row: camera image masked by entropy thresholding and image with gradient energy, Bottom row: binary image and resulting line-segments.

In figure 2 the main results of the preprocessing stage are shown.

B. Image to World Transformation

The transformation from image to world coordinates serves a number of purposes. On the one hand geometrical relationships can be easily evaluated in world coordinates, on the other hand parametric lane border estimation is remarkable simplified in this domain. Furthermore, the world coordinate system is a reasonable domain for fusing data, that stem from different sensors.

The image to world mapping makes use of the constraints given in the context of driver assistance systems and is described in [16] in detail. The mapping requires the vanishing line to be horizontal in the image, and the points mapped are assumed to lie on a plane (ground plane constraint). Due to space limitations, here we only depict an extension, which is aimed at coping with rotations of the vehicle.

It can be shown, that the angle between the projection of the optical axis onto the ground plane and the linear

[1] In order to save computation time, the local entropy image is efficiently estimated by making use of sampling and quantization techniques.

lane borders is given by

$$\phi(t) = \tan^{-1}(k_x \frac{v_x(t-1) - x_c}{k_{y1}}) \,. \qquad (1)$$

The constants k_x, k_{y0}, k_{y1} are derived from the projections of the standardized road markings (see [16]), x_c is the horizontal image coordinate of the center of projection, and $v_x(t-1)$ denotes the horizontal image coordinate of the intersection of the linear lane borders (estimated in the previous time step) with the horizon. By rotating the world coordinates by the angle $\phi(t)$ the linear parts of the lane borders are parallel to vertical world coordinate axis independent of the vehicle's actual orientation. Therefore, lane changes result in a horizontal shift of the world coordinates. This effect significantly simplifies parametric lane border estimation in the world domain.

C. Vehicle Detection

In vision based driver assistance systems the vehicle detection task is usually divided in a segmentation and a subsequent tracking stage. Obviously, the results obtained by segmentation algorithms and the tracking module are not independent. Therefore, we have built a coupling architecture, aiming to suppress false detections and thereby to increase the reliability of the whole vehicle detection stage. In our system we implemented two different vehicle segmentation algorithms, which are based on different image features.

The first segmentation algorithm employs the line-segments calculated in the preprocessing stage for generating a list of potential vehicle positions. The middle of each approximately horizontal segment serves as a starting position for searching lateral vehicle borders. Two signals are calculated by vertically projecting image and gradient data in an image area defined by the line-segment and the expected height of the vehicle. The lateral borders of a potential vehicle are determined by thresholding the signals obtained by the projection. If the vehicle's width matches the expected width at the given image position (estimated in the lane-detection module), the ROI (region of interest) is accepted.

The second strategy for detecting potential vehicle positions utilizes the lane border estimates, i.e., is based on higher-level knowledge. The outline of the algorithm is as follows: Each lane is scanned from the lowest image row to a certain vertical coordinate that corresponds to a predefined maximal distance in the world. Potential vertical vehicle positions are obtained if a certain number of pixel in a row (delimited by the lane borders) exceed a significant vertical gradient level. In order to accept or to reject the hypotheses obtained by scanning the rows, the same test for lateral vehicle borders as in the segmentation module I is performed.

We take advantage of the redundant information provided by the different segmentation algorithms by temporal integration and coupling with an object tracker. The tracker we employ is based on the Hausdorff-Distance [17] and is described in [18] in detail. But instead of calculating the distance transform on the basis of the features as given in [18] the corner image obtained in the preprocessing stage is used. In figure 3 the integrating architecture

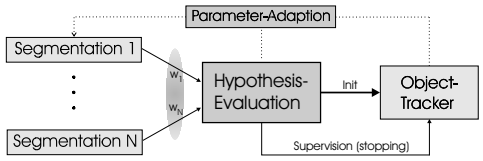

Fig. 3. Architecture for the integration of initial segmentation results and the coupling with an object tracker. The dotted lines indicate a potential feedback for online adapting the coupling weights and the internal parameters of the segmentation algorithms.

is depicted. The basic integration of evidence for a certain vehicle hypothesis is carried out similar to the confidence integration as performed in the lane-detection module (see section II-D).

This coupling mechanism can be considered as a list of object hypotheses integrating or removing evidence depending on space and time. The resulting vehicle detection module consisting of the two segmentation algorithms and the hypothesis integration mechanism proved to outperform the single algorithms by suppressing false detections.

D. Lane Detection

A number of tasks such as lane departure warning and lane following rely on the information about the vehicle's position relative to the lane boundaries. Due to the importance of lane-detection much research has been done in this field [10], [19], [20].

Reasonable approaches to lane-detection have to incorporate a bottom-up process detecting new lane borders and a lane tracking process based on the previously detected lane positions. In order to efficiently perform the bottom-up process, we utilize the line-segments for generating lane hypotheses. To remove the effects induced by the perspective projection, the line-segments pointing to an estimated vanishing point are transformed to world-coordinates. A list of lane hypotheses is generated by evaluating projections of the transformed line-segments onto the horizontal world coordinate axis. Each lane hypothesis $H_i(t) = \{ C_i(t), c_{0,i}(t), c_{1,i}(t), c_{2,i}(t) \}$, $1 \leq i \leq n^H(t)$ consists of a confidence level C_i, and the lane parameters $\vec{c}_i = [c_{0,i}, c_{1,i}, c_{2,i}]^T$. The lane parameters are the coefficients of a polynomial

$$x^L_{w,i}(y_w) = c_{0,i} + c_{1,i}\, y_w + c_{2,i}\, y_w^2 \qquad (2)$$

modeling the lane border in world coordinates [2]. We chose the polynomial model, because the estimation of the linear coefficients c_0, c_1, c_2 can be performed more efficiently than e.g. estimating a true clothoidal shape.

The coupling between the bottom-up lane detection and the tracking mechanism is effectively carried out at the hypotheses level. Each potential lane position $\tilde{c}_{0,j}$ detected

[2]The origin of the world coordinate system corresponds to the image pixel (x_c, h), where h denotes the lowest image row.

by the bottom-up process is compared to the list of previously obtained hypotheses $H_i(t-1), 1 \le i \le n^H(t-1)$. If $|\tilde{c}_{0,j}(t) - c_{0,i}(t-1)| > \delta_L$ for all i (i.e., the $\tilde{c}_{0,j}$ cannot be assigned to any existing hypothesis) a new hypothesis $H_k(t) = \{C_k(t) = C^0, c_{0,k}(t) = \tilde{c}_{0,j}(t), c_{1,k}(t) = c_{2,k}(t) = 0\}$ is generated. The parameter δ_L defines the maximal distance between corresponding lateral lane positions, and C^0 is the confidence initially assigned to new hypotheses. A hypothesis i is regarded as evident if $C_i(t)$ exceeds the threshold δ_C. For each evident hypothesis an oriented search for lane border points based on the lane parameters $c_{0,i}(t-1), c_{1,i}(t-1), c_{2,i}(t-1)$ estimated in the previous time step is performed. Therefore the functional form of equation 2 is transformed to image coordinates [3]

$$
\begin{aligned}
K_0 &= \frac{1}{2c_2 k_x \sin^2\phi} && (3)\\
K_1 &= 2c_2(x_c k_x \sin\phi - k_{y1}\cos\phi)K_0 \sin\phi && (4)\\
K_2 &= (1 - 2c_2 k_{y0}\sin\phi)K_0\cos\phi - c_1 K_0 \sin\phi && (5)\\
K_3 &= K_0^2(\cos\phi - c_1\sin\phi)^2 - 4c_2 K_0^2(k_{y0} + c_0\sin\phi)\sin\phi && (6)\\
K_4 &= -4c_2 k_{y1} K_0^2 \sin\phi && (7)\\
x^L(y) &= K_1 + K_2(y - v_y) - \sqrt{(K_3(y-v_y)+K_4)(y-v_y)}\,. && (8)
\end{aligned}
$$

When a hypothesis becomes evident for the first time, the parameters $c_{1,i}(t-1), c_{2,i}(t-1)$ are not available; instead the line-segments projecting into the cluster, which corresponds to the hypothesis, define the initial search positions in the image. The result of the local search is the matrix

$$
P_i(t) = \begin{bmatrix} x_{w,1}(t) & x_{w,2}(t) & x_{w,3}(t) & \dots & x_{w,n_p}(t) \\ y_{w,1}(t) & y_{w,2}(t) & y_{w,3}(t) & \dots & y_{w,n_p}(t) \end{bmatrix}^T \qquad (9)
$$

containing the detected lane points transformed to world coordinates. On the basis of $P_i(t)$ the parameters $c_{0,i}(t-1), c_{1,i}(t-1), c_{2,i}(t-1)$ are updated by a weighted recursive least square (RLS) algorithm [21]. In order to make the RLS-algorithm robust against horizontal shift of the world coordinate system (e.g., in case of lane change) the a-priori error

$$
\begin{aligned}
e_i(t, t-1) &= \frac{1}{n_p}\sum_{\nu=1}^{n_p} e_{i,\nu}(t, t-1) && (10)\\
e_{i,\nu}(t, t-1) &= x_{w,\nu}(t) - \vec{y}_{w,\nu}^T(t)\,\vec{c}_i(t-1) && (11)\\
\vec{y}_{w,\nu}(t) &= [\,1 \;\; y_{w,\nu}(t) \;\; y_{w,\nu}^2(t)\,]^T && (12)
\end{aligned}
$$

is added to the parameter $c_{0,i}$ prior to the application of the RLS-algorithm. After the estimation of the lane parameters the confidence levels C_i are updated by the following dynamics:

$$
\begin{aligned}
\frac{d\,C_i(t)}{dt} &= -\frac{1}{\tau}C_i(t) + f_{D,i}(t) + f_{T,i}(t) && (13)\\
f_{D,i}(t) &= \begin{cases} 0 & \text{if } |\tilde{c}_{0,j}(t) - c_{0,i}(t-1)| > \delta_L \;\forall\, j \\ \gamma_D & \text{else.} \end{cases} && (14)\\
f_{T,i}(t) &= \gamma_T e^{-\gamma_2\left(\frac{1}{n_p}\sum_{\nu=1}^{n_p} e_{i,\nu}^2(t,t-1) - e_i^2(t,t-1)\right)} && (15)
\end{aligned}
$$

By equation 13 evidence is integrated on the basis of the results of the bottom-up detection (f_D) and the results of the lane tracking process (f_T). The function f_T is a measure for the correspondence of the detected lane points $P_i(t)$ with the lane estimate at $t-1$, and depends on the variance of the a-priori error. If f_D and f_T evaluate to zero, i.e. the hypothesis does not receive any support, the confidence $C_i(t)$ decreases exponentially in time. The main advantage of additive confidence calculation as given by equation 13 is, that further contributions, e.g., obtained by texture analysis, can be easily integrated.

[3] v_y denotes the vertical image coordinate of the horizon.

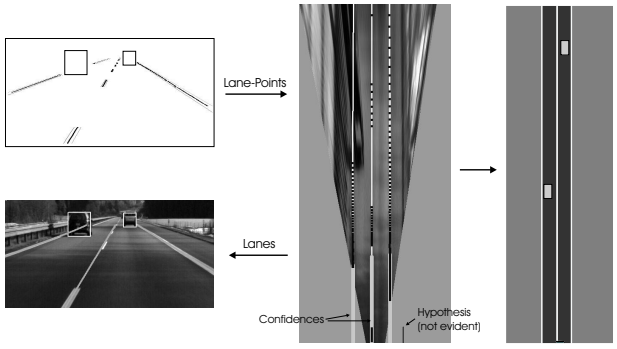

Fig. 4. Lane points detected in the camera image, transformed to world coordinates, and subsequent parametric lane estimation. Image areas corresponding to detected vehicles are not taken into account when searching for lane points. In contrast to the lane points the camera image is transformed only for visualization purposes. On the right hand side the observed scene is depicted in a symbolic bird's eye view.

Some driver assistance tasks such as lane departure warning and lane following are based on the vehicles position relative to the lane borders. We propose the vehicles lateral offset from the lane center normalized by the current lane width as an appropriate measure:

$$
\vartheta_V(t) = \frac{c_{0,R}(t) + c_{0,L}(t)}{2(c_{0,R}(t) - c_{0,L}(t))} \qquad (16)
$$

The indices L and R correspond to the vehicles inner left and right lane borders. The dynamics of $\vartheta_V(t)$ can be learned in order to operate a lane change warning system in consideration of the current driver's behaviour.

Results

The image processing system has been successfully tested on a variety of traffic scenes, including different weather and lightning conditions. Due to the lack of any benchmark databases to which different systems could be compared, it is not possible to directly compare different systems. In figure 5 the camera image, the detected lanes and vehicles, as well as the lateral offset $\vartheta_V(t)$ are depicted. The example sequence demonstrates that the shadows do not cause any problems; furthermore it can be seen that $\vartheta_V(t)$ and therefore the lane borders are determined robustly. The total mean computation time per frame (496x256 pixel, Pentium III, 1Ghz) computed on this sequence is 42ms, whereas the preprocessing stage takes 32ms. Due to the high level preprocessing features, the whole domain specific processing, i.e., the vehicle segmentation, the tracking and intermediate hypotheses evaluation, as well as the lane detection, are computed within 10ms.

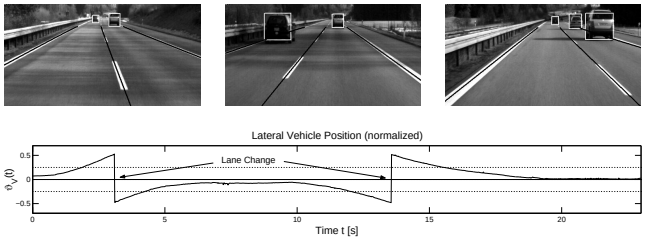

Fig. 5. Results of the image processing system tested on a sequence of 1440 images (24 seconds, 60Hz). The plot shows the normalized lateral vehicle offset $\vartheta_V(t)$ with respect to the middle of the current lane. The images are taken at $t = 2.4$s, $t = 11.5$s and $t = 19.5$s.

E. Detection of Non Rigid Objects

In recent years, not much attention has been given to image processing approaches aimed at increasing the safety of more passive and exposed traffic participants such as pedestrians and motorcyclists, respectively, in urban environments. A major goal is to perform a judgement on object behaviour to forestall collision of a moving observer equipped with such a driver assistant system. The work presented here addresses the localization of pedestrians.

Pedestrian recognition

The initial detection and the tracking of pedestrians in urban environments faces several problems such as cluttered backgrounds, roads in bad condition and large object movements. The objects themselves are non-rigid and can change their appearance on a very short time scale. Also highly varying pose, self-occlusion and the occurrence of pedestrians in groups call for new object representations.

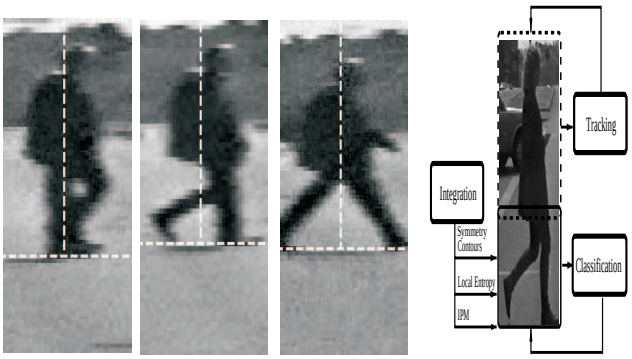

Fig. 6. Concept for recognition of pedestrians. Illustrated is the local dynamic integration of features for the initial detection, the tracking of the main torso based on different features and the limb movement analysis as a cue for the final classification.

Besides other recently introduced approaches to pedestrian recognition [22], [23], [24] in [25] the initial detection process is based on a fusion of texture analysis, model-based contour grouping (see figure 6), the geometric features of pedestrians, and inverse-perspective mapping (IPM) [26] (binocular vision). Additionally, in [25] motion patterns of limb movements have been analyzed to verify object hypotheses (see figure 6). The tracking of the quasi-rigid part of the body is performed by different algorithms that have been successfully employed for the tracking of sedans, trucks, motorbicycles, and pedestrians. The Hausdorff-distance [18], [6] has been applied both to the tracking of objects and template matching of limbs of moving bodies. The final recognition is based on a temporal correlation analysis of the walking process. Recently, in [27], a symmetry operator, which groups morphological preprocessing results, has been applied to initial hypothesis generation at locations of vertical image structure. Furthermore, stereo calculations aim at determining a more accurate distance measure. A final head and shoulder template match also aims at recognizing pedestrians viewed from a frontal or back view. In [28] a more general and flexible approach is introduced, which takes a closer look at body part identification in cooperation with human detection. In that application, initial detection of contour outline sets are based on a stereo segmentation. Furthermore the idea of recursively matching a translation, rotation and scale invariant human model onto image data in a Bayesian reasoning framework seems to be very appealing. This model is rich in that it takes into account aspects of body part self-occlusion, and also different viewing angles.

Symmetry Detection

In our approach, image features are chosen very carefully under the aspects of generality and simplicity. They should be invariant under a wide range of conditions so that the same detection and tracking framework will function well in a broad variety of situations. Also in an effort to make object detection and tracking as efficient as possible the features should be easy to extract. In addition, our new symmetry operator brings together the ideas of representing the image data compactly by means of skeletonization with continuous edge information and also in the same run to encode also gray scale color and form information. Therefore, a local symmetry detector has been developed, which compactly encodes and groups locally symmetric image structure. This attention like processing step of the system allows a very rapid scene analysis for further processing steps of higher resolution. This aspect has recently also been proposed within the MIT pedestrian detection system [24] in [29].

For the initial detection we constrain the symmetry operator just to compute symmetry information between edges of opposite polarity. One interesting property is that while scanning over the whole image in an exhaustive way that both the mean of the gray-scale distribution and the distance between the strongest edges of opposite polarity is instantaneoulsy encoded. A framework similar to ours is the one developed for robust image correspondences using a radial cumulative similarity transform [30].

Local symmetric image structure is grouped along traces from the local symmetry operator output to parametric ellipses. The ellipses then encode the mean distance between the contributing edges and the mean of the gray scale distribution of the original underlying image. Also the mean

orientation of each symmetry segment is encoded by the starting and end point of the ellipses. To deal with ambiguities, symmetry segment traces are built at different levels of feature resolution and threshold selection. For the initial detection weak assumptions, determining the strength of the connectivity criteria of elements to be grouped, have been chosen.

Hypothesis generation

For further processing, initial foot points of objects are detected by vertically scanning up the image from local maxima of down-projected vertical symmetry values (see figure 7). Also, the bottom of symmetry ellipse clusters with symmetry area close to the expected object size yield further foot points. Of course, within a suggested region of interest we also deal with over and under-segmentation of image structure. Therefore, to apply high domain model knowledge, we follow up similar approaches as those mentioned in [28] to recursively correct contour segmentation errors through a hierarchical localization procedure using compactly encoded higher domain model knowledge. The difference of our methodology to previous ones is that the shift to a reference coordinate system, suggested by a strong symmetry axis, and the instantaneous image structure segmentation is a step towards replacing recent presegmentation stages totally relying on the performance of stereo segmentation. It should be pointed out that our framework is already capable to detect relevant body part structure in the far field and does not depend on strong dynamics in scene depth, which is a common requirement for standard stereo algorithms to work well.

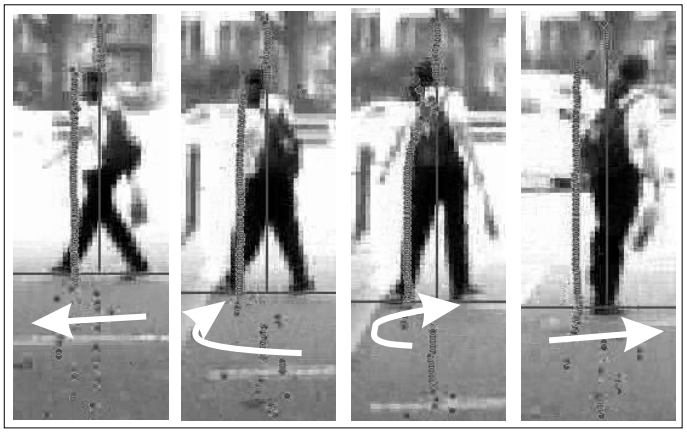

Fig. 7. Complex scene of an interaction of a moving observer with a pedestrian in urban environments. This local turning action of a pedestrian should demonstrate, that spontaneous actions lower the prediction horizon of an observer. Since 2D stereo algorithms are not well suited for object segmentation, especially in the very far field, we estimate sparse stereo information along the symmetry axis of object hypothesis. Results are illustrated by the dotted disparity values at automatically generated object hypothesis locations. For the refinement of the height of initial bounding boxes we obtain rough estimates for the object height at locations where disparity values significantly depart from the disparity mean, robustly estimated in the initial bounding box.

The main goal of a dynamic hypotheses tracking framework is to associate independently detected objects coherently over time and instantaneously classify situations, e.g. such as illustrated in figure 7 of a pedestrian's spontaneous change of walking direction, being detected and tracked from a moving observer. Also, based on an invariant object-representation w.r.t. ego-motion induced by the moving observer, classification can now be guided by real world trajectory identification of the objects of interest, similar to those methods, recently published in [31]. Being able to map all information of the object domain into a low dimensional temporal framework will allow us to predict risky situations and forestall obstacle collision within a very short time scale.

F. Context-Based Object Detection

In this section, a general, domain-independent, stochastic model-based approach for an automated scene analysis is presented. The approach consists of an initial segmentation, in which the image is divided into a set of disjoint regions based on their respective color values and a subsequent joint classification where the generated image regions are assigned to object classes. Here we concentrate on the presentation of the classification process. For details about the segmentation and classification see [32], [33]. Within the classification not only isolated image regions are considered, but a whole ensemble of image regions. To improve reliability the classification process is performed as a fusion of sensor information and symbolic information. Context knowledge, defined as knowledge about the spatial relationships between the different object classes, is used as an example for symbolic information. We provide a general framework to carry out the fusion in a systematic, unified way including a methodology of expressing symbolic information analytically with the help of Markov random field theory [34].

Joint classification

The goal of the classification process is to assign one of a predefined number of object classes to every image region. In addition to sensor information in the form of extracted regional features like color, size or texture, symbolic information is used to generate the assignment. In our approach the classification is formulated as an optimization problem using a maximum a posteriori estimation rule. The classification criteria are combined using the Bayesian theorem, where feature measurements and symbolic information are coded as conditional probability and a-priori probability, respectively [33], [35]. Several strategies exist for deriving a probabilistic expression coding the assignment dependent on the feature measurements. To restrict the model complexity we choose a simple Gaussian observation model with zero mean and a covariance matrix of diagonal form. To get an analytical expression for symbolic information coded as a-priori probability we used a Markov random field model-based approach. With its associated Gibbs distribution a systematic methodology for representing symbolic information using properly designed

clique functions is provided. For more details see [32].

Having derived analytical expressions for modeling object features as well as symbolic information the optimization functional is completely defined. Among all possible values of the assignment, the one which maximizes the a posteriori probability is sought. The optimization task is solved by applying an evolutionary algorithm. This has proven to be a very efficient search strategy thanks to a problem related formulation of the mutation operators guiding the evolutionary process.

Results

The presented approach has been tested on different video sequences showing typical scenarios of road traffic on motor-ways. The initial segmentation has been performed on the basis of object color. We used a clustering approach for image segmentation which was adapted by modifying the underlying probability distribution to improve segmentation results [32], [33]. In the classification process we used region color in the feature based part of the optimization functional.

To demonstrate the benefit of our approach we compare the classification results based only on feature measurements with the results obtained when using context in addition. We discuss the results on the basis of the following example image.

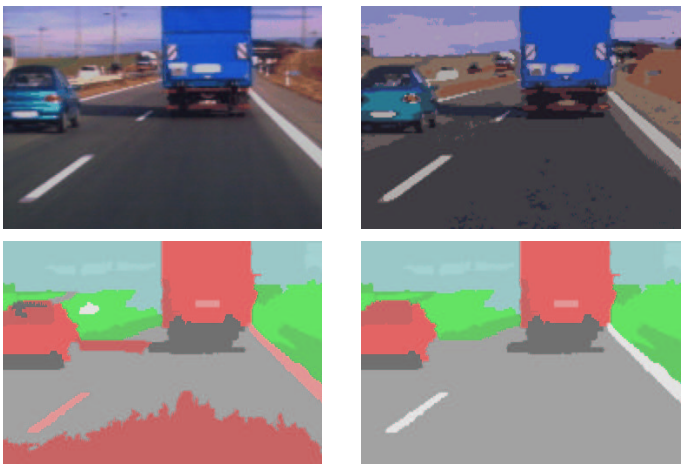

Fig. 8. Results of different processing steps within the classification process. In the first row the original true color image and the segmentation result can be seen. In the second row the classification results without and under consideration of context are shown. The colors in the last image denote the assignment of the image regions to different object classes: red marks the object class "vehicle", dark gray the object class "shadow", light gray the object class "street", white, green and blue the object classes "lane marking", "vegetation" and "sky", respectively.

The image in figure 8 show the original true color image, the segmentation result and the classification results without and with context. Here, we are especially interested in the classification results. The image shows that the utilization of context significantly improves the classification result. Incorrect assignments due to similar feature configurations of different object classes can be considerably diminished. All vehicles and most of the street, sky and vegetation regions are accurately identified.

III. Representation

The object information obtained by the image processing stage must be fused with data stemming from other sensors to reach a common description of the sensed environment. To be able to efficiently implement different behaviour warning or generation tasks, this common representation is essential. In the following, we will present an approach to sensor data fusion that is based on an array of Kalman-Filters.

For tracking purposes, Kalman Filters have long been employed, and their theory is well-established [36]. They are well-suited for the tracking of single objects where the number of state vector components is fixed. The main problem in using them in traffic scene analysis is establishing the correspondence between the signals of the various sensors and the objects they might be referring to.

In order to achieve robust sensor integration based on a physical model of movement without the need to previously establish sensor/object relationships, an approach of sensor fusion by using an array of Kalman Filters has been developed. Every cell of the spatially organized Kalman Filter array consists of separate Kalman Filters for the x- and y-parameters of movement, as well as an additional scalar excitation value:

$$\underbrace{\text{Parameters for } x, \dot{x}, \ddot{x}}_{\hat{\vec{x}}, \mathbf{P_x}} \quad \underbrace{\text{Parameters for } y, \dot{y}}_{\hat{\vec{y}}, \mathbf{P_y}} \quad \underbrace{\alpha}_{\text{global excitation}} \tag{17}$$

In our case, the tracked state variables of the Kalman Filters are x, $\dot{x}$, $\ddot{x}$, y and $\dot{y}$, where x is the relative position of potential obstacles in longitudinal direction, and y in lateral direction. The separation of the state vectors into independent ones for x- and y-direction is convenient for efficiency reasons. An additional element of each cell is a weight α which serves as a reliability measure.

The actual sensor data are coupled into this array at a location based on their spatial measurement. The various Kalman Filters experience the usual observational and temporal updates. The entire process is depicted in figure 9. Instead of explicit state vectors $\vec{x}$ and their covariances $\mathbf{P_x}$ we employ a square root information form [36, p. 260] using $\mathbf{C_{Y_x}}$ and $\vec{S}_x$ instead.

The novel part in the depicted data flow of the Kalman Filter array is the spatial coupling of the individual Kalman Filters. The information of each Kalman Filter contributes in the same manner as actual measurements to its neighbors' state vectors. The actual process employed is geoverned by a discrete variant of diffusion. The weights used for the diffusion are calculated according to the ratio of probabilities the Kalman Filter's parameters (mean and covariance of a normal distribution) indicate for an object at the current and adjacent cell positions, and the Kalman Filter's state vector is used as observational input according to those weights. Due to the diffusion process,

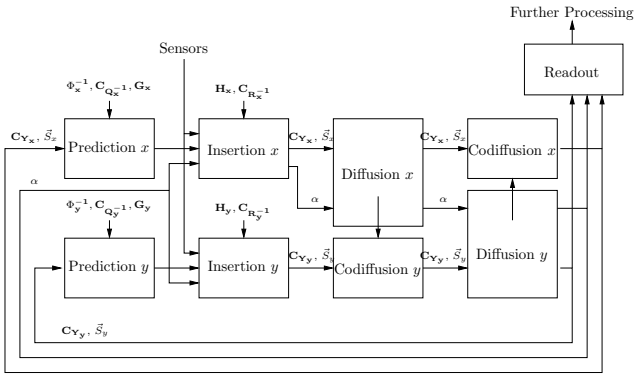

Fig. 9. Data flow in the Kalman Filter array.

the activation of the Kalman array tends to gravitate to the spatial position indicated by it, and will do so even in the case of missing input if the Kalman Filter parameters correspond to an object in movement. The information for a coherent object will spread out according to the distribution indicated by the Kalman Filter parameters, with weights α that are proportional to the corresponding normal distribution. For stationary inputs corresponding to a single object, the output will be equivalent to that of a single Kalman Filter.

(a) Camera image, back view. Rotate 180° to match orientation of graphics to the right.

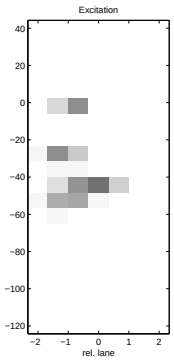

(b) Excitation α

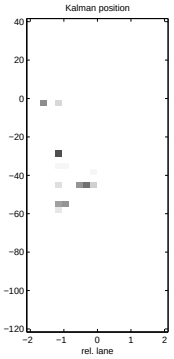

(c) Positional histogram

Fig. 10. Traffic scene with camera image, excitation of the Kalman Filter array and histogram of indicated positional parameters of the filters. In b), dark cells indicate high reliability and excitation of the corresponding filter.

Results

As a demonstration of the performance, we show the distribution of excitation values α in a traffic application (cf. fig. 10(b)) as well as an α-weighted histogram (cf. fig. 10(c)) of the indicated object positions. It is obvious that in spite of the somewhat loose information distribution and the comparatively coarse raster used for the Kalman Filter array, the actual interpreted data quite sharply indicate the separate objects.

The proposed structure is thus capable of exploiting both spatial and temporal redundancies for sensor fusion. It can track the movement of objects continuously, since the raster of the Kalman Filter array does not constrict the spatial resolution, but merely the possibility for discriminating among adjacent different objects.

IV. Behaviour Generation

The information about the environment as observed by various sensors and fused in the Kalman-Filter array must be evaluated in order to fullfil the demanded system task. As pointed out, there are a number of different tasks a driver assistance system can be devoted to. We believe, that if a system is capable of autonomous driving, the development of a variety of driver assistance tasks will be much simplified. This is due to the possibility of comparing actual driving manoeuvres with potential actions as would be initiated by the system.

In the following, we present an approach to autonomous driving that has been developed and tested within a simulated environment. The trajectory of the vehicle can be learned by evolutionary optimization of the Neural Field parameters controlling the trajectory generation.

A. Behaviour Generation by Neural Fields

The aim of a system for behaviour generation in traffic situations is to produce a secure, continuous, and comfortable trajectory of the guided vehicle. This behaviour is characterized by the intended behaviour and the state of the environment. The trajectory is generated by the dynamics of the control variables *steering angle* and *velocity*. The intended behaviour is influenced by the development of the current traffic situation, by physical constraints, traffic rules and intentions of the driver. Those different kinds of information have to be evaluated to result in an appropriate behaviour of the vehicle.

Publications dealing with the task of behaviour generation mostly concentrate on the control of either steering angle [37], [8] or velocity [38], [39]. Fully automated driving changing both controlled variables was proposed by [40] in a project of truck platooning where Kalman Filtering is used for steering. In [41] an expert system for generating driving behaviour is proposed. A first application of Neural Fields for behaviour generation was published in [42] for intelligent cruise control. There, the steering angle and the velocity are determined by the evaluation of Neural Field excitations. That system is specialized on following a leading vehicle.

The behaviour generating system proposed here introduces a different approach to vehicle control. The concept is characterized by a separation of a planning and an action level, where the planning level induces a motivation for a movement into the action-level. The system aims at controlling a vehicle autonomously or partly autonomously. Information concerning the actual situation and its development, the actual task, traffic rules and technical constraints are used to generate a smooth, task-relevant trajectory. All levels are realized by nonlinear dynamics: Neural Fields [43] and decision dynamics [44], [45].

On the planning level all information concerning medium-termed actions are integrated into nonlinear dynamics to decide for a goal-position. The goal-position is used to determine the motivation which forces the movement of the vehicle into the corresponding direction. To achieve this effect the motivation is coupled into the action-level. The action-level determines the controlled variables. It is designed for obstacle avoidance in face of the motivation. Therefore, the shift of movement towards the goal-position is interrupted if it is demanded by the current situation. The action-level is realized by Neural Field dynamics to generate a smooth trajectory and to evaluate the situation determined by other traffic participants and the street course. The motivation is introduced into the Neural Fields by influencing an asymmetric interaction of field-sites [46], which results in a movement that can be stopped by an input signal.

As the behaviour of a vehicle has to be determined in dependence of the relative lane positions and longitudinal distances, the behaviour generation system operates on the basis of lateral (y-) and longitudinal (x-) coordinates.

A.1 Results

The behaviour generating system successfully navigates the vehicle through different traffic situations of varying complexity in a simulated environment. One result is presented for a complex situation affording different kinds of reactions. The situation is described in figure 11. The resulting position and velocity values are shown in figure 12. At first the reference vehicle changes to the middle lane to evade the slower vehicle in the right lane. The vehicle cannot change to the outer left lane until the faster vehicle comming from behind has passed. Therefore, the car must decrease its velocity to avoid the slower vehicle in the middle lane (fig. 12 at $t = 12$s). After the vehicle on the left lane has passed, it changes lanes to the left, overtakes the car in the middle lane and reaches the desired velocity. Then it returns to the right lane as soon as possible as demanded by the traffic rules. The complex behavioural sequence is successfully finished.

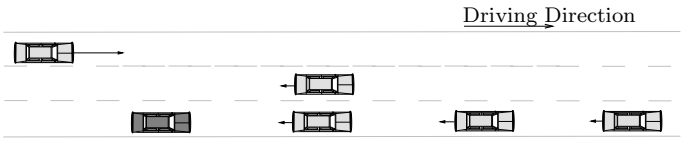

Fig. 11. Bird's eye view of a simulated traffic situation as a test of behaviour generation. The reference vehicle (black, 25m/s) is trying to adopt the desired speed (first 28m/s after 10s 33m/s) which is larger than the speed of the four cars (25m/s) in front. From the back on the left lane a faster vehicle (35m/s) is approaching. Relative velocities are indicated by black arrows.

The system is tested in a simulation environment. Even in complex traffic situations the system is able to produce smooth trajectories obeying the traffic rules and avoiding dangerous situations. The sub-symbolic implicit formulation as continuous coupled dynamics seamlessly integrates rules, motivations and sensor inputs. The dynamic variables and the dynamics' time scales have been selected in accordance with the behaviour to generate and the inertia of the vehicles. The usage of real sensor data is not yet possible as the view of the scene changes with the steering of the vehicle. This behaviour cannot be predicted in detail by a former real driver collecting sensor data.

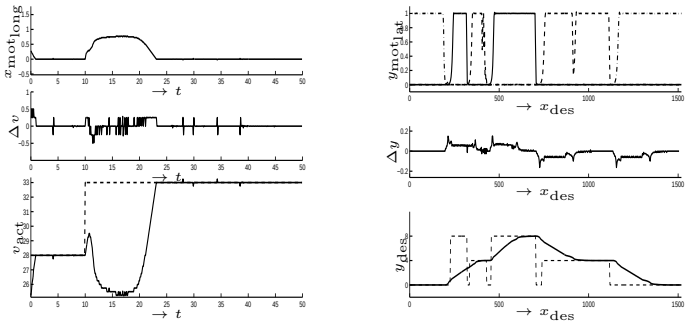

(a) Long. Motivation and Velocity (b) Lateral Motivation and world position

Fig. 12. Resulting time course of the motivation and control dynamics. The dashed lines show the actual motivated value of the desired velocity value and lane position.

B. *Optimization of Neural Fields for Trajectory Generation*

When dealing with dynamic neural field models the question of how to adjust the model parameters arises. This problem can be solved using gradient-based learning, evolutionary optimization, or hybrid approaches, cf. [47]. For complex tasks, we favor evolutionary algorithms (EAs). Here we employ a state-of-the-art evolution strategy, the CMA-ES [48], [49], [26] for optimizing the car trajectory during a lane change [50].

In the previous sections, we have shown the functionality of driver assistance for automatic cruise control based on neural field dynamics. For additional actions initiated by the driver, e.g., an active lane change, this methodology can be adapted. The main advantage of the neural field approach—the additional input characteristic—is preserved in this formalism. Not only the desired lane but also obstacles hindering the lane change can be taken into account.

Considering a lane change the leader- and the lane-stimulus are replaced by one stimulus representing the center of the desired lane. In case of no disturbing objects a "correct" lane change has to be performed. In our context the term "correct" means that changes in the steering angle result in a smooth trajectory which comforts the driver. The trajectory is determined by the parameters of the field dynamics. We optimized the parameters of the system so that the car trajectory comes close to a given trajectory that we regard as optimal. This trajectory could be extracted from real lane change manoeuvres. The fitness function measures the differences between desired and actual trajectory. As the neural field model is translation-invariant, only a single test scenario is needed (for a given speed). The fitness function is not differentiable, so only direct optimization methods are applicable. After the evo-

lutionary adaption, the differences between desired and actual trajectory nearly vanished.

V. Conclusions and Outlook

Although the state of soft-computing applications has improved recently, the development of driver assistance systems remains a challenging task. The difficulty arises from the demand, that such systems must reliably interpret the physical measurements delivered by various sensors and generate the intended behaviour on that basis. In order to cope with the resulting complexity such systems must be organized by a modular, hierarchical architecture. We presented such a modular architecture defining four levels of data processing, by which an increasing amount of symbolic information is gained sequentially.

Image data is our main source of information about the environment. We propose to calculate a meaningful high level feature basis, that once calculated is accessed by the different specific processing modules. The calculated features not only increase the robustness of the higher level modules with respect to varying lightning conditions, but also the computational efficiency of the whole image processing stage. Operating on these features we propose approaches to lane, vehicle and pedestrian detection. An additional image segmentation and region classification approach is presented, allowing us to integrate context knowledge into the classification process.

If sensors like RADAR or LIDAR provide additional information about the environment, their measurements should be fused with the results of the image processing stage. This can be achieved by the presented spatially coupled array of Kalman-Filters. This approach provides a common world coordinate system based scene representation that can be accessed by the modules realizing the intended driver assistance task. In our view, a universal scene representation, not relying on the actual system task, will simplify the development of a number of different Intelligent Vehicles applications.

We also presented our work on autonoumos driving. In our approach a coupling between planning (motivation) and action level is proposed. The coupling as well as well as the representation of task relevant information is carried out by means of Neural Fields and decision dynamics. By doing so, the system is capable of interrupting initiated manoeuvres if indicated by the sensor data.

In the future we plan to further improve parts of the presented system components. In the lane detection module texture analysis may help to distinguish outer lane borders from straight structures causing lane hypotheses. Also, when no road markings are available, texture based approaches may provide a mean for detecting lane border points. We plan to enhance our vehicle detection strategy by online adapting the parameters and the corresponding weights of the segmentation algorithms. This shall be achieved by feeding back the results of the object tracker and comparison with the output of the segmentation algorithms. Also, further work will concentrate on pedestrian recognition. Here, the focus is put on the dynamical integration of various image features.

In order to be able to implement and test different behaviour generation strategies, we are currently developing a highway traffic simulation environment. Within this artificial environment a number of cars (agents) will autonomously act in consideration of surrounding vehicles, the intended velocity, traffic rules, and physical constraints. We also plan to integrate an OpenGL based sensor data simulation that will provide camera images from arbitrary perspectives. This framework will provide a link between the sensor data processing and the behaviour generation stage. The Neural Field based behaviour generation system is currently converted to C++, in order to be tested within the simulation environment.

Acknowledgments

Parts of the presented work were developed within a number of industry cooperations. The authors would like to acknowledge the support of the BMBF under grant LOKI 01 IB 001 C, BMW AG, Adam Opel AG, Siemens AG, and Infineon AG.

References

[1] M. Bertozzi and A. Broggi, "GOLD: A Parallel Real-Time Stereo Vision System for Generic Obstacle and Lane Detection," *IEEE Transactions on Image Processing*, vol. 7, no. 1, pp. 62–81, January 1998.

[2] T.N. Tan, G.D. Sullivan, and K.D. Baker, "Model-based Localization and Recognition of Road Vehicles," *International Journal of Computer Vision*, vol. 27, no. 1, pp. 5–25, March 1998.

[3] C. Curio, J. Edelbrunner, T. Kalinke, C. Tzomakas, and W. von Seelen, "Walking Pedestrian Recognition," in *ITSC*, Tokyo, Japan, 1999, pp. 292–297, IEEE.

[4] U. Handmann, T. Kalinke, C. Tzomakas, M. Werner, and W.v. Seelen, "An Image Processing System for Driver Assistance," in *Proceedings of the IEEE Conference on Intelligent Vehicles*, Stuttgart, Germany, 1998, pp. 481–486, IEEE.

[5] F. Thomanek, E.D. Dickmanns, and D. Dickmanns, "Multiple Object Recognition and Scene Interpretation for Autonomous Road Vehicle Guidance," in *Proceedings of the Intelligent Vehicles '94 Symposium, Paris, France*, 1994, pp. 231–236.

[6] C. Tzomakas, *Contributions to the Visual Object Detection and Classification for Driver Assistance Systems , PhD Thesis*, Shaker Verlag, 1999.

[7] T. Kalinke, *Texturbasierte dynamische Erkennung veränderlicher Objekte*, Ph.D. thesis, Institut für Neuroinformatik, Ruhr-Universität Bochum, Germany, VDI-Verlag, 1999.

[8] A. Broggi, M. Bertozzi, A. Fascioli, and G. Conte, *Automatic Vehicle Guidance: The Experience of The ARGO Autonomous Vehicle*, World Scientific Co. Publisher, 1999.

[9] C. Thorpe, Ed., *Vision and Navigation*, The Carnegie Mellon Navlab. Kluwer Academic Publishers, Boston, Mass., 1990.

[10] E. D. Dickmanns and B. D. Mysliwetz, "Recursive 3-d Road and relative ego-state Recognition," *IEEE Transactions on Pattern Analysis and Machine Intelligence*, vol. 14, no. 2, pp. 199–213, 1992.

[11] Rudolf Gregor and E. D. Dickmanns, "EMS-Vision: Mission Performance on Road Network," in *Procs. IEEE Intelligent Vehicles Symposium 2000*, Detroit, USA, Oct. 2000, pp. 140–145.

[12] Martin Pellkofer and E. D. Dickmanns, "EMS-Vision: Gaze Control in Autonomous Vehicles," in *Procs. IEEE Intelligent Vehicles Symposium 2000*, Detroit, USA, Oct. 2000, pp. 296–301.

[13] M. Luetzeler and E. D. Dickmanns, "EMS-Vision: Recognition of Intersections on Unmarked Road Networks," in *Procs. IEEE Intelligent Vehicles Symposium 2000*, Detroit, USA, Oct. 2000, pp. 302–307.

[14] M. Betke, E. Haritkaoglu, and L. Davis, "Real-time multiple

vehicle detection and tracking from a moving vehicle," *Machine Vision and Applications*, , no. 12, pp. 69–83, 2000.
[15] J.F. Canny, "A computational approach to edge detection," *IEEE Transactions on Pattern Analysis and Machine Intelligence*, vol. 8, pp. 679–698, November 1986.
[16] T. Bücher, "Measurement of Distance and Height in Images based on easy Attainable Calibration Parameters," in *Procs. IEEE Intelligent Vehicles Symposium 2000*, Detroit, USA, Oct. 2000, pp. 314–319.
[17] D.P. Huttenlocher, G.A. Klanderman, and W.J. Rucklidge, "Comparing Images Using the Hausdorff Distance," *IEEE Transactions on Pattern Analysis and Machine Intelligence*, vol. 15-9, pp. 850–863, 1993.
[18] M. Werner, *Objektverfolgung und Objekterkennung mittels der partiellen Hausdorff-Distanz*, Fortschritt-Berichte VDI, Reihe 10, Nr. 574, 1999.
[19] A. Broggi and S. Berte, "Vision-based road detection in automotive systems: A real time expectation-driven approach," *Journal of Artificial Intelligence Research*, pp. 325–348, 1995.
[20] Axel Gern, Uwe Franke, and Paul Levi, "Advanced Lane recognition - fusing vision and radar," in *Procs. IEEE Intelligent Vehicles Symposium 2000*, Detroit, USA, Oct. 2000, pp. 45–51.
[21] S. Haykin, *Adaptive Filter Theory*, Information and System Sciences. Prentice Hall, Englewood Cliffs, second edition, 1991.
[22] C. Wöhler, J. Anlauf, T. Pörtner, and U. Franke, "A Time Delay Neural Network Algorithm for Real-Time Pedestrian Recognition," in *Proceedings of IV*, 1998, pp. 247–252.
[23] L. Zhao and C. Thorpe, "Stereo and Neural Network-Based Pedestrian Detection," in *ITSC99*, 1999, pp. 289–303.
[24] C. Papageorgiou, T. Evgeniou, and T. Poggio, "A Trainable Pedastrian Detection System," in *Proceedings of IV*, 1998, pp. 241–246.
[25] C. Curio, J. Edelbrunner, T. Kalinke, C. Tzomakas, and W. von Seelen, "Walking Pedestrian Recognition," *Special Issue of IEEE Transactions on Intelligent Transportation Systems, (Tokyo, Japan)*, vol. 1, pp. 155–163, 2000.
[26] T. Bergener, C. Bruckhoff, and C. Igel, *Imaging and Vision Systems: Theory, Assessment and Applications*, chapter Parameter Optimization for Visual Obstacle Detection using a Derandomized Evolution Strategy, Advances in Computation: Theory and Practice. NOVA Science Books, Huntington, NY 11743 (USA), 2001.
[27] A. Broggi, M. Bertozzi, A. Fascioli, and M. Sethi, "Shape-based Pedestrian Detection," in *Procs. IEEE Intelligent Vehicles Symposium 2000*, Detroit, USA, Oct. 2000.
[28] L. Zhao and C. Thorpe, "Recursive context reasoning for human detection and part identification," in *IEEE Workshop Workshop on Human Modeling, Analysis, and Synthesis*, 2000.
[29] F. Miaua, Papageorgiou, and L. Itti, "Neuromorphic algorithms for computer vision and attention," in *Proceedings SPIE 46 Annual International Symposium on Optical Science and Technology*, 2001.
[30] T. Darrell, "A radial cumulative similarity transform for robust image correspondence," in *Proceedings of the Conference on Computer Vision and Pattern Recognition*, 1998, pp. 656–662.
[31] R. Rosales and S. Sclaroff, "Trajectory guided tracking and recognition actions," Tech. Rep., BU-CS- 99-002, Boston University, 1999.
[32] G. Lorenz, *Ein farb- und kontextbasierter Ansatz zur Objekterkennung*, ibidem-Verlag, 2001, Phd-Thesis.
[33] G. Lorenz, "Using topological constraints as context for the joint classification of image regions in a traffic environment," in *Proceedings of the ITSC*, 2001.
[34] S.Z. Li, *Markov random field modeling in computer vision*, Springer-Verlag, 1995.
[35] J.W. Modestino and J. Zhang, "A Markov Random Field Model-Based Approach to Image Interpretation," *IEEE Transactions on Pattern Analysis and Machine Intelligence*, vol. 14, no. 6, pp. 606–615, 1992.
[36] Mohinder S. Grewal and Angus P. Andrews, *Kalman Filtering*, Prentice Hall, 1993.
[37] S. Tsugawa, H. Mori, and S. Kato, "A Lateral Control Algorithm for Vision-Based Vehicles with a Moving Target in the Field of View," in *IEEE International Conference on Intelligent Vehicles*, Stuttgart, Germany, 1998, vol. 1, pp. 41–45, IEEE Industrial Electronics Society.
[38] Q. Zhuang, J. Gayko, and M. Kreutz, "Optimization of a Fuzzy Controller for a Driver Assistant System," in *Proceedings of the Fuzzy-Neuro Systems 98*, München, Germany, 1998, pp. 376 – 382.
[39] U. Handmann, I. Leefken, and C. Tzomakas, "A Flexible Architecture for Intelligent Cruise Control," in *ITSC'99, IEEE Conference on Intelligent Transportation Systems 1999*, Tokyo, Japan, 1999.
[40] U. Franke, F. Böttiger, Z. Zomotor, and D. Seeberger, "Truck platooning in mixed traffic," in *Symposium on Intelligent Vehicles 1995*, Detroit, USA, 1995.
[41] R. Sukthankar, *Situation Awareness for Tactical Driving*, Phd thesis, Carnegie Mellon University, Pittsburgh, PA, United States of America, 1997.
[42] U. Handmann, I. Leefken, A. Steinhage, and W. v. Seelen, "Behavior Planning for Driver Assistance using Neural Field Dynamics ," in *Second international symposium on 'Neural Computation'*, Berlin, Germany, 2000, NC 2000.
[43] S.I. Amari, "Dynamics of pattern formation in lateral inhibition type neural fields," *Biological Cybernetics*, vol. 27, pp. 77–87, 1977.
[44] A. Steinhage, "The Dynamic Approach to Anthropomorphic Robotics," in *Controlo 2000*, 2000.
[45] T. Bergener and A. Steinhage, "An Architecture for Behavioral Organization using Dynamic Systems," in *German Workshop on Artificial Life*, GWAL'98, Ed., 1998.
[46] K. Zhang, "Representation of spatial orientation by the intrinsic dynamics of the head-directed cell ensemble: A theory," *Journal of Neuroscience*, vol. 16, pp. 2112–2126, 1996.
[47] C. Igel, W. Erlhagen, and D. Jancke, "Optimization of neural field models," *Neurocomputing*, vol. 36, no. 1-4, pp. 225–233, 2001.
[48] N. Hansen and A. Ostermeier, "Convergence properties of evolution strategies with the derandomized covariance matrix adaptation: The $(\mu/\mu, \lambda)$-CMA-ES," in *EUFIT'97, 5th European Congress on Intelligent Techniques and Soft Computing*, Aachen, 1997, pp. 650–654, Verlag Mainz, Wissenschaftsverlag.
[49] N. Hansen and A. Ostermeier, "Completely derandomized self-adaptation in evolution strategies," *Evolutionary Computation*, vol. 9, no. 2, pp. 159–195, 2001.
[50] H. Edelbrunner, U. Handmann, C. Igel, I. Leefken, and W. von Seelen, "Application and optimization of neural field dynamics for driver assistance," in *The IEEE 4th International Conference on Intelligent Transportation Systems, ITSC '01.* 2001, IEEE Press.